PERGAMON

International Journal of Solids and Structures 39 (2002) 5225–5240

INTERNATIONAL JOURNAL OF SOLIDS and STRUCTURES

www.elsevier.com/locate/ijsolstr

The application of the Eshelby equivalent inclusion method for unifying modulus and transformation toughening

Zhonghua Li *, Lihong Yang

School of Civil Engineering and Mechanics, Shanghai Jiaotong University, Shanghai Minhang 200240, PR China

Received 25 November 2001; received in revised form 10 July 2002

Abstract

When a crack is lodged in an inclusion, both difference between the modulus of the inclusion and matrix material and stress-free transformation strain of the inclusion will cause the near-tip stress intensity factor to be greater (amplification effect) or less (shielding or toughening effect) than that prevailing in a homogeneous material. In this paper, the inclusion may represent a second phase particle in composites and a transformation or microcracked process zone in brittle materials, which may undergo a stress-free transformation strain induced by phase transformation, microcracking, thermal expansion mismatch and so forth. A close form of solution is derived for predicting the toughening (or amplification) effect. The derivation is based on Eshelby equivalent inclusion approach that provides rigorous theoretical basis to unify the modulus and transformation contributions to the near-tip field. As validated by numerical examples, the developed formula has excellent accuracy for different application cases.

Keywords: Eshelby equivalent inclusion approach; Stress intensity factor; Microcrack toughening; Transformation toughening

1. Introduction

Microcracking in a process zone near macrocrack tip has been observed in many brittle materials (Ruehle et al., 1987; Hueber and Jillek, 1977; Knehans and Steinbrech, 1982; Hoaland and Embury, 1980). It was found that the process zone may postpone the outset of unstable macroscopic crack propagation and is a viable toughening mechanism (Evans and Mater, 1988; Evans and Faber, 1986; McMeeking and Evans, 1982; Hutchinson, 1987; Evans and Cannon, 1986). Toughening arises from two consequences of microcracking, reduction in modulus and dilatational strain due to release of residual stress. The present theoretical analyses (McMeeking and Evans, 1982; Hutchinson, 1987; Evans and Cannon, 1986) treat the microcrack process zone as a dilatational particle with reduction in modulus, and establish considerable similarities between transformation toughening and microcrack toughening, by relating the change in

* Corresponding author. Tel.: +86-2154743918; fax: +86-54743044.
E-mail address: zhli@sjtu.edu.cn (Z. Li).

0020-7683/02/$ - see front matter © 2002 Elsevier Science Ltd. All rights reserved.
PII: S0020-7683(02)00420-1

toughness to the permanent dilatation and the reduced modulus in the process zone. The former is often called the transformation toughening, and latter the modulus toughening.

The stress-induced transformations which can cause significant toughening include martensitic and ferroelastic (Evans and Mater, 1988; Clussen et al., 1984) transformations, as well as twinning. The former involves both dilatational and shear components of the transformation strain, while the latter typically have only a shear component. Considerable toughness enhancement is observed in ceramic systems strengthened by tetragonal zirconia (ZrO_2) particles which transform martensitically to monoclinic crystal structure, resulting in a shear strain of about 16% and a dilatation of 4% (Hoaland and Embury, 1980; Evans and Mater, 1988; Evans and Faber, 1986; McMeeking and Evans, 1982). It is well known that variation in crystal structure will, in general, change the elastic modulus of the transformation zone (Kriven, 1990).

In addition, if crack tip is partially penetrating a second phase particle in composite materials, it will, in most cases, have different modulus and coefficients of thermal expansion compared with matrix material. An appreciable misfit strain will then develop on cooling from fabrication temperature or during variation in environmental temperature (Withers et al., 1989).

Therefore, in most cases the modulus and transformation toughening take place inevitably at the same time. They should be regarded as two cooperative processes. Hence, a method, which can unify the modulus toughening and transformation toughening, is of general significance.

However, the present model for transformation toughening (McMeeking and Evans, 1982; Lambropoulos, 1986; Budiansky et al., 1983) is developed based on the assumption that the transformation zone and matrix material have same elastic constants. A close form of solution to modulus toughening is given by Hutchinson (1987). However, it is limited to the lowest order effect of the modulus difference between inclusion and matrix material. Furthermore, it was assumed that the modulus and transformation contributions can be simply superimposed. The interaction effects between them are not yet investigated.

The toughening mechanisms of the modulus and transformation toughening essentially are the same, both resulting in mismatch strains between inclusion and matrix material. Since the analysis of the transformation toughening for homogeneous inclusion (McMeeking and Evans, 1982) is based on Eshelby inclusion technique, it is natural to treat the toughening problem for inhomogeneous inclusion by the Eshelby equivalent inclusion technique.

In this paper, we treat the problem in a more general case: the inclusion surrounding crack-tip may represent a transformation or microcracking process zone, or a second phase particle as the crack partially penetrating it. The inclusion may undergo some degree of stress-free transformation strain, such as induced by phase transformation, thermal expansion mismatch, or release of residual stress as microcrack forming. Both the modulus difference between inclusion and matrix material and the transformation strain will cause the near-tip stress intensity factor (SIF) to be greater (amplification effect) or less (shielding effect) than that prevailing in a homogeneous material. However, for convenience of description in the present paper, we use the term of toughening to present both the amplification and shielding effects. We first develop a method to unify the modulus and transformation toughening based on Eshelby equivalent inclusion technique. Then several applications to modulus and transformation toughening as well as the interaction effects between them will be discussed.

2. Mode and formulation

As shown in Fig. 1(a), the crack tip is located within an inclusion, which may have an arbitrary shape, but is symmetrical with respect to the crack plane. The inclusion undergoes a stress-free transformation strain, $\mathbf{e}^{T^*}$. The Young's modulus and Poisson's ratio of the inclusion, E_I and ν_I, differ from those of the matrix material, E_M and ν_M. It is assumed that the size of the inclusion is small compared with crack length

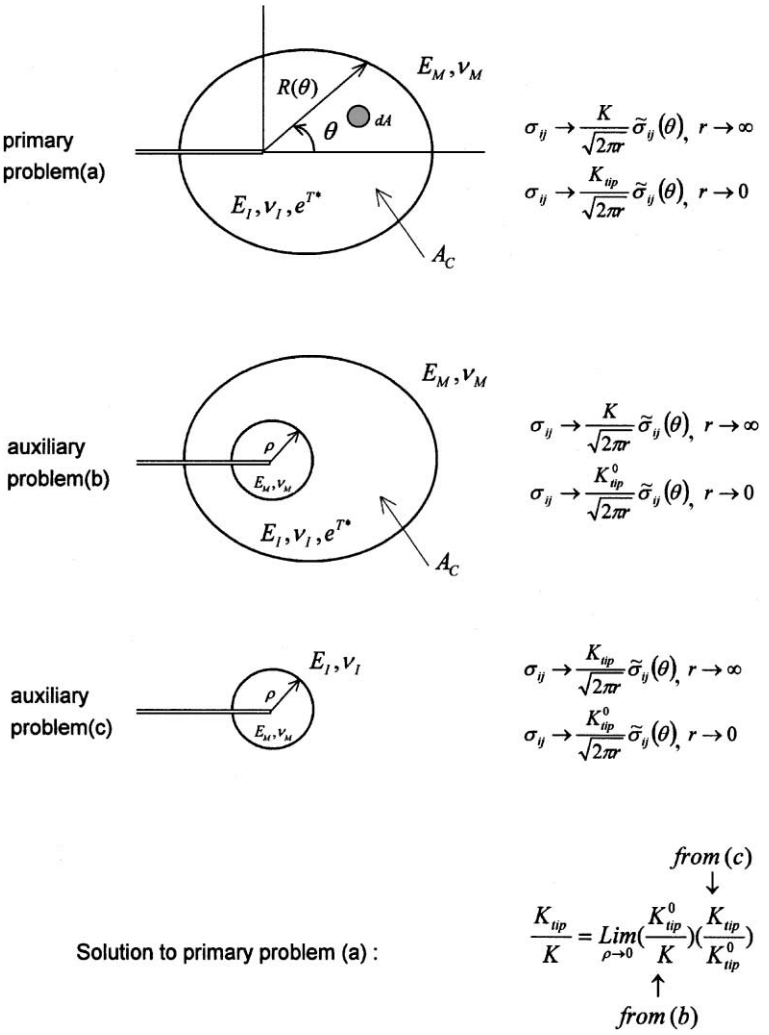

Fig. 1. Definitions of auxiliary problems (b) and (c) and their use in construction of the solution to the primary problem (a).

and other dimensions of the crack body. Therefore, the inclusion is within applied remote K-field and the near-tip fields have the same form, denoted by K_{tip}:

$$\sigma_{ij} = \frac{K}{\sqrt{2\pi r}}\tilde{\sigma}_{ij}(\theta) \quad r \to \infty \tag{2.1}$$

$$\sigma_{ij} = \frac{K_{\text{tip}}}{\sqrt{2\pi r}}\tilde{\sigma}_{ij}(\theta) \quad r \to 0 \tag{2.2}$$

Now, we consider a differential element dA within the inclusion, which undergoes a stress-free transformation strain, $\mathbf{e}^{\mathrm{T}^*}$, simultaneously sustains an applied strain field $\mathbf{e}^{\mathrm{A}}$, exerted by the remote stress intensify K. The equivalent transformation strain in dA, $\mathbf{e}^{\mathrm{T}}$, is given by

$$\mathbf{e}^{\mathrm{T}} = [(\mathbf{C}_{\mathrm{I}} - \mathbf{C}_{\mathrm{M}})\mathbf{S} + \mathbf{C}_{\mathrm{M}}]^{-1}[(\mathbf{C}_{\mathrm{M}} - \mathbf{C}_{\mathrm{I}})\mathbf{e}^{\mathrm{A}} + \mathbf{C}_{\mathrm{I}}\mathbf{e}^{\mathrm{T}^*}] \tag{2.3}$$

according to Eshelby equivalent inclusion approach (Withers et al., 1989; Eshelby, 1957), where $\mathbf{S}$ is the Eshelby tensor, dependent solely upon the inclusion shape and the Poisson's ratio of the matrix material. $\mathbf{C}_I$ and $\mathbf{C}_M$ are the elastic tensors of the inclusion and matrix material, respectively. As shown in (2.3), the equivalent transformation strain $\mathbf{e}^T$ in dA varies with the applied strain $\mathbf{e}^A$, and is not zero for an inhomogeneous inclusion ($C_I \neq C_M$) even when $\mathbf{e}^{T^*} = 0$.

The Eshelby approach is mathematically rigorous for an infinite matrix containing a single ellipsoidal inclusion. When the inclusion undergoes a uniform stress-free transformation strain, the stress and strain within the inclusion are uniform. However, in order to utilize the approach in more realistic situations, there has been considerable activity in extending Eshelby approach to various problems, such as the interaction of two ellipsoidal inclusions (Moschobidis and Mura, 1975), the behavior of hybrid composite (Taya and Chou, 1981) and short fibre reinforced composites (Withers et al., 1989), the calculation of the stress field inside a nonellipsoidal inclusion which are not uniform (Johnson et al., 1980), to cite only a few examples. In the present study, we extend the Eshelby approach to the case of an inclusion with arbitrary shape embedded in crack-tip field. Either the nonellipsoidal shape of the inclusion considered or the singular crack-tip field will result in a nonuniform stress–strain field within the inclusion. However, we assume that the Eshelby theory can be used to each differential element within the inclusion, which undergoes uniform transformation strain determined by (2.3) and the resultant stresses in which are uniform. Then a nonuniform transformation strains, therefore also the stresses, inside the inclusion, can be obtained by integrating (2.3) in the domain of the inclusion.

For simplicity, it is assumed that the inclusion and matrix material are isotropic and their Poisson's ratios are the same, denoted by v. Then we have

$$\mathbf{C}_I = \alpha \mathbf{C}_M \tag{2.4}$$

where

$$\alpha = E_I / E_M \tag{2.5}$$

Combining (2.3) and (2.4), it gives

$$\mathbf{e}^T = \mathbf{e}^{TA} + \mathbf{e}^{Te} = \mathbf{L}\mathbf{e}^A + \mathbf{T}\mathbf{e}^{T^*} \tag{2.6}$$

where

$$\mathbf{L} = [(\alpha - 1)\mathbf{S} + \mathbf{I}]^{-1}(1 - \alpha) \tag{2.7}$$

$$\mathbf{T} = \alpha[(\alpha - 1)\mathbf{S} + \mathbf{I}]^{-1} \tag{2.8}$$

Here, $\mathbf{I}$ is the identity tensor. Thus, the tensor $\mathbf{L}$ and $\mathbf{T}$ relate, respectively, the equivalent transformation strain $\mathbf{e}^T$ in the inclusion to the applied strain $\mathbf{e}^A$, and the inherent transformation strain $\mathbf{e}^{T^*}$ without going into the details of the form of the $\mathbf{C}_I$ and $\mathbf{C}_M$ tensors. The first term in the right hand side of (2.6) is the equivalent transformation strain induced by the applied strain, denoted by $\mathbf{e}^{TA}$ for the inhomogeneous inclusion. It is zero for homogeneous inclusion ($\mathbf{C}_I = \mathbf{C}_M$). The second term in the right hand side of (2.6) is the equivalent transformation strain induced by the inherent transformation strain $\mathbf{e}^{T^*}$ of the inclusion, denoted by $\mathbf{e}^{Te}$, which is equal to the $\mathbf{e}^{T^*}$ for homogeneous inclusion, but depends upon $\mathbf{C}_I$ and $\mathbf{C}_M$ for inhomogeneous inclusion. According to transformation toughening theory (Knehans and Steinbrech, 1982; Hoaland and Embury, 1980), the increment in SIF due to the differential element with transformation strain $\mathbf{e}^T$ defined in (2.6) is given by

$$dK^0_{tip} = \frac{1}{2\sqrt{2\pi}} \frac{E_M}{1 - v^2} r^{-3/2} \Omega(e^T_{\alpha\beta}, \theta)\, dA \tag{2.9}$$

for plane strain mode I crack, where

$$\Omega(e^{\mathrm{T}}_{\alpha\beta},\theta) = (e^{\mathrm{T}}_{11}+e^{\mathrm{T}}_{22})\cos\frac{3\theta}{2} + 3e^{\mathrm{T}}_{12}\cos\frac{5\theta}{2}\sin\theta + \frac{3}{2}(e^{\mathrm{T}}_{22}-e^{\mathrm{T}}_{11})\sin\theta\sin\frac{5\theta}{2} \tag{2.10}$$

It is essential to note that Eq. (2.9) is derived for the case that the transformation area have the same modulus with its surrounding. Therefore, the elastic modulus E_{M} used in (2.9), and the K^0_{tip} is the SIF for the crack tip within a medium of same modulus as matrix materials, not the desired factor K_{tip} for the case shown in Fig. 1(a).

It can be seen from (2.6) that the equivalent transformation strains contributed from applied load and inherent transformation strain can be simply superimposed for an inhomogeneous inclusion. Hence, their contributions to the variation in the SIF can be separately evaluated.

To obtain the K_{tip}/K solution for the primary problem in Fig. 1(a), we adopt the method developed by Hutchinson (1987). The solution is constructed using solutions to two auxiliary problems denoted by (b) and (c) in Fig. 1. Once the solutions to the two auxiliary problems are in hand, the ratio of the SIF sought is given by

$$\frac{K_{\mathrm{tip}}}{K} = \left(\frac{K^0_{\mathrm{tip}}}{K}\right) \Big/ \left(\frac{K^0_{\mathrm{tip}}}{K_{\mathrm{tip}}}\right) \tag{2.11}$$

where K^0_{tip}/K is the ratio of the near-tip to remote intensity factor in the auxiliary problem (b), and $K^0_{\mathrm{tip}}/K_{\mathrm{tip}}$ is the corresponding ratio in the auxiliary problem (c).

The solution to the auxiliary problem (b) can be written down immediately using (2.9)

$$\frac{K^0_{\mathrm{tip}}}{K} = 1 + \frac{E_{\mathrm{M}}}{2\sqrt{2\pi}(1-\nu^2)K}\int_A r^{-3/2}\Omega(e^{\mathrm{T}}_{\alpha\beta},\theta)\,\mathrm{d}A \tag{2.12}$$

where the area integral extends over the upper half of A_{c}, excluding the inner circular region.

To generate the solution to auxiliary problem (c), Hutchinson exploited a special region A_{c} for which K_{tip}/K is known. The special region A_{c} is the infinite strip with a centered semi-infinite crack shown in Fig. 2. From a simple energy argument or application of the J-integral (see (3.22) in the next section for the case of $\nu_{\mathrm{I}} = \nu_{\mathrm{M}}$) the following relation holds

$$\frac{K_{\mathrm{tip}}}{K} = \sqrt{\alpha} \tag{2.13}$$

exactly for this problem. Then by evaluating K^0_{tip}/K for this special mode, one can "back-out" the desired universal result $K^0_{\mathrm{tip}}/K_{\mathrm{tip}}$ for the auxiliary problem (c) used in (2.11). The details for evaluating $K^0_{\mathrm{tip}}/K_{\mathrm{tip}}$ for the auxiliary problem (c), and K^0_{tip}/K for the auxiliary problem (b) will be given in the following section.

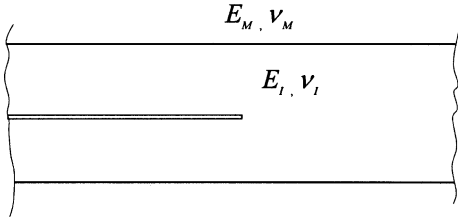

Fig. 2. Spherical geometry used to be infer solution to auxiliary problem (c) shown in Fig. 1.

3. The crack-tip stress intensity factor

Throughout this paper, it is assumed that the size of the inclusion is small compared with the length of the crack. Under this condition the applied strain field to the inclusion shown in Fig. 1 is that of the mode I crack controlled by the remote SIF K

$$\left.\begin{aligned} e_{11}^{A} &= \frac{K}{E_M\sqrt{2\pi r}}(1+v)\cos\frac{\theta}{2}\left[(1-2v)-\sin\frac{\theta}{2}\sin\frac{3\theta}{2}\right] \\ e_{22}^{A} &= \frac{K}{E_M\sqrt{2\pi r}}(1+v)\cos\frac{\theta}{2}\left[(1-2v)+\sin\frac{\theta}{2}\sin\frac{3\theta}{2}\right] \\ e_{12}^{A} &= \frac{K}{E_M\sqrt{2\pi r}}(1+v)\cos\frac{\theta}{2}\sin\frac{\theta}{2}\cos\frac{3\theta}{2} \\ e_{33}^{A} &= e_{13}^{A} = e_{23}^{A} = 0 \quad \text{for plane strain} \end{aligned}\right\} \tag{3.1}$$

For a differential element with circular section inside A_c, the components of the Eshelby tensor are given by Mura (1987)

$$\left.\begin{aligned} S_{1111} &= S_{2222} = \frac{5-4v}{8(1-v)}, \quad S_{1122} = S_{2222} = \frac{4v-1}{8(1-v)} \\ S_{1133} &= S_{2233} = \frac{v}{2(1-v)}, \quad S_{1212} = \frac{3-4v}{4(1-v)} \\ S_{1313} &= S_{2323} = \frac{1}{2} \end{aligned}\right\} \tag{3.2}$$

And other components are zero. Substituting (3.2) into (2.7) and (2.8), it gives

$$\left.\begin{aligned} L_{1111} &= L_{2222} = \frac{(1-\alpha)(1-v)(3-4v+5\alpha-4v\alpha)}{(1+\alpha-2v)(1+3\alpha-4v\alpha)} \\ L_{1122} &= L_{2211} = -\frac{(1-\alpha)^2(1-v)(1-4v)}{(1+\alpha-2v)(1+3\alpha-4v\alpha)} \\ L_{1133} &= L_{2233} = \frac{(1-\alpha)^2 v}{(1+\alpha-2v)}, \quad L_{3333} = (1-\alpha) \\ L_{1212} &= \frac{4(1-\alpha)(1-v)}{(1+3\alpha-4v\alpha)}, \quad L_{1313} = L_{2323} = \frac{2(1-\alpha)}{1+\alpha} \end{aligned}\right\} \tag{3.3}$$

and

$$\left.\begin{aligned} T_{1111} &= T_{2222} = \frac{\alpha(1-v)(3-4v+5\alpha-4v\alpha)}{(1+\alpha-2v)(1+3\alpha-4v\alpha)} \\ T_{1122} &= T_{2211} = \frac{\alpha(1-\alpha)(1-v)(1-4v)}{(1+\alpha-2v)(1+3\alpha-4v\alpha)} \\ T_{1133} &= T_{2233} = \frac{\alpha(1-\alpha)v}{(1+\alpha-2v)}, \quad T_{3333} = \alpha \\ T_{1212} &= \frac{4\alpha(1-v)}{(1+3\alpha-4v\alpha)} \\ T_{1313} &= T_{2323} = \frac{2\alpha}{(1+\alpha)} \end{aligned}\right\} \tag{3.4}$$

Other components of the **L** and **T** tensors are zero.

The transformation strains used in (2.12) are determined by (2.6)

$$\left.\begin{aligned} e_{\alpha\alpha}^{\mathrm{TA}} &= (L_{1111}+L_{1122})(e_{11}^{\mathrm{A}}+e_{22}^{\mathrm{A}}) = \frac{4(1-\alpha)(1-2v)(1-v^2)K}{(1+\alpha-2v)E_{\mathrm{M}}\sqrt{2\pi r}}\cos\frac{\theta}{2} \\ e_{22}^{\mathrm{TA}}-e_{11}^{\mathrm{TA}} &= (L_{1111}-L_{1122})(e_{22}^{\mathrm{A}}-e_{11}^{\mathrm{A}}) = \frac{4(1-\alpha)(1-v^2)K}{(1+3\alpha-4v\alpha)E_{\mathrm{M}}\sqrt{2\pi r}}\sin\theta\sin\frac{3\theta}{2} \\ e_{12}^{\mathrm{TA}} &= L_{1212}e_{12}^{\mathrm{A}} = \frac{2(1-\alpha)(1-v^2)K}{(1+3\alpha-4v\alpha)E_{\mathrm{M}}\sqrt{2\pi r}}\sin\theta\cos\frac{3\theta}{2} \end{aligned}\right\} \tag{3.5}$$

$$\left.\begin{aligned} e_{\alpha\alpha}^{\mathrm{Te}} &= (T_{1111}+T_{1122})(e_{11}^{\mathrm{T}^*}+e_{22}^{\mathrm{T}^*}) = C_3(e_{11}^{\mathrm{T}*}+e_{22}^{\mathrm{T}^*}) \\ e_{22}^{\mathrm{Te}}-e_{11}^{\mathrm{Te}} &= (T_{1111}-T_{1122})(e_{22}^{\mathrm{T}^*}-e_{11}^{\mathrm{T}*}) = C_4(e_{22}^{\mathrm{T}*}-e_{11}^{\mathrm{T}*}) \\ e_{12}^{\mathrm{Te}} &= T_{1212}e_{12}^{\mathrm{T}*} = C_5e_{12}^{\mathrm{T}*} \end{aligned}\right\} \tag{3.6}$$

Substituting (3.5), (3.6) and (2.10) into (2.12), we have

$$\frac{K_{\mathrm{tip}}^0}{K} = 1 + C_1\beta_1 + C_2\beta_2 + (C_3\beta_3 + C_4\beta_4 + C_5\beta_5)/K \tag{3.7}$$

where

$$C_1 = \frac{(1-\alpha)(1-2v)}{(1+\alpha-2v)} \tag{3.8}$$

$$C_2 = \frac{3(1-\alpha)}{2(1+3\alpha-4v\alpha)} \tag{3.9}$$

$$C_3 = C_5 = \frac{4\alpha(1-v)}{(1+3\alpha-4v\alpha)} \tag{3.10}$$

$$C_4 = \frac{2\alpha(1-v)}{(1+\alpha-2v)} \tag{3.11}$$

$$\beta_1 = \frac{1}{\pi}\int_0^{\pi} \ln[R(\theta)]\cos\frac{\theta}{2}\cos\frac{3\theta}{2}\,\mathrm{d}\theta \tag{3.12}$$

$$\beta_2 = \frac{1}{\pi}\int_0^{\pi} \ln[R(\theta)]\sin^2\theta\cos\theta\,\mathrm{d}\theta \tag{3.13}$$

$$\begin{aligned} \beta_3 &= \frac{E_{\mathrm{M}}}{2\sqrt{2\pi}(1-v_2)}(e_{11}^{\mathrm{T}*}+e_{22}^{\mathrm{T}*})Lim_{\rho\to 0}\int_0^{\pi}\cos\frac{3}{2}\theta\,\mathrm{d}\theta\int_{\rho}^{R(\vartheta)} r^{-1/2}\,\mathrm{d}r \\ &= \frac{E_{\mathrm{M}}}{\sqrt{2\pi}(1-v^2)}(e_{11}^{\mathrm{T}*}+e_{22}^{\mathrm{T}*})\int_0^{\pi} R(\theta)^{1/2}\cos\frac{3}{2}\theta\,\mathrm{d}\theta \end{aligned} \tag{3.14}$$

$$\begin{aligned} \beta_4 &= \frac{3E_{\mathrm{M}}}{2\sqrt{2\pi}(1-v^2)}e_{12}^{\mathrm{T}*}Lim_{\rho\to 0}\int_0^{\pi}\sin\theta\cos\frac{5}{2}\theta\,\mathrm{d}\theta\int_{\rho}^{R(\vartheta)} r^{-1/2}\,\mathrm{d}r \\ &= \frac{3E_{\mathrm{M}}}{\sqrt{2\pi}(1-v^2)}e_{12}^{\mathrm{T}*}\int_0^{\pi} R(\theta)^{1/2}\sin\theta\cos\frac{5}{2}\theta\,\mathrm{d}\theta \end{aligned} \tag{3.15}$$

$$\beta_5 = \frac{3E_M}{4\sqrt{2\pi}(1-\nu_2)}(e_{22}^{T*} - e_{11}^{T*})Lim_{\rho\to 0}\int_0^{\pi} \sin\theta \sin\frac{5}{2}\theta \,d\theta \int_{\rho}^{R(\vartheta)} r^{-1/2}\,dr$$
$$= \frac{3E_M}{2\sqrt{2\pi}(1-\nu_2)}(e_{22}^{T*} - e_{11}^{T*})\int_0^{\pi} R(\theta)^{1/2}\sin\theta\sin\frac{5}{2}\theta\,d\theta \tag{3.16}$$

Since the integral $\int_0^{\pi}\cos(\theta/2)\cos(3\theta/2)\,d\theta = 0$ and $\int_0^{\pi} C_2\sin^2\theta\cos\theta d\theta = 0$ in (3.12) and (3.13), the β_1 and β_2 are independent of the radius of the inner circular core ρ. It can be also seen that β_1 and β_2 are unchanged when $R(\theta)$ is replaced by $\lambda R(\theta)$ and are thus dependent on the shape, but not on the size of the inclusion.

We return to the problem shown in Fig. 2. The integral in the definitions of $\beta_1 \sim \beta_5$ are easily evaluated for this geometry ($\beta_1 = 0.5$, $\beta_2 = -0.125$, $\beta_3 = \beta_4 = \beta_5 = 0$). Then, the solution to the auxiliary problem (b) for this geometry is given by

$$\frac{K_{tip}^0}{K} = 1 + 0.5C_1 - 0.125C_2 \tag{3.17}$$

from (2.13) and (3.17), one immediately obtains the solution for the auxiliary problem (c) shown in Fig. 1(c).

$$\frac{K_{tip}^0}{K_{tip}} = \frac{1 + 0.5C_1 - 0.125C_2}{\sqrt{\alpha}} \tag{3.18}$$

By combining (3.7) and (3.18) according to (2.11), the general solution for the primary problem shown in Fig. 1(a) can be finally given by

$$\frac{K_{tip}}{K} = \frac{\sqrt{\alpha}[1 + \beta_1 C_1 + \beta_2 C_2 + (C_3\beta_3 + C_4\beta_4 + C_5\beta_5)/K]}{1 + 0.5C_1 - 0.125C_2} \tag{3.19}$$

To obtain an explicit solution, it is assumed in the previous derivation that the Poisson's ratios of the inclusion and matrix material are the same. This assumption sets a limit to apply the Eq. (3.19) for more general case. However, this limitation may be relaxed by introduction a modified factor. The J-integral from integration contours that circle the crack tip lying outside inclusion is given by

$$J = (1 - \nu_M^2)K^2/E_M \tag{3.20}$$

while the J-integral for all such contours lying inside inclusion

$$J_{tip} = (1 - \nu_I^2)K_{tip}^2/E_I \tag{3.21}$$

Then one obtains

$$\frac{K_{tip}}{K} = \sqrt{\frac{J_{tip}\alpha}{J}\frac{(1-\nu_M^2)}{(1-\nu_I^2)}} \tag{3.22}$$

for plane strain condition.

For the case of $\nu_I = \nu_M$, (3.19) and (3.22) are identical if the effect of the inclusion on J can be neglected. This is true because we have assumed that the remote stress–strain field is controlled by K, i.e., the perturbation of the small inclusion on the remote K-field is neglected. Consequently, (3.19) and (3.22) leads to a modified factor $((1-\nu_M^2)/(1-\nu_I^2))^{1/2}$ in (3.19)

$$\frac{K_{tip}}{K} = C_0[1 + C_1\beta_1 + C_2\beta_2 + (C_3\beta_3 + C_4\beta_4 + C_5\beta_5)/K] \tag{3.23}$$

where

$$C_0 = \frac{1}{1 + 0.5C_1 - 0.125C_2}\sqrt{\frac{\alpha(1-\nu_M^2)}{1-\nu_I^2}} \tag{3.24}$$

for the case of $\nu_I \neq \nu_M$. It should be noted that the Poisson's ratio used in $C_1 \sim C_5$ is ν_M because $C_1 \sim C_5$ are derived from the remote stain field. As well be seen in following section, the modified formula (3.23) gives good approximation for the case of $\nu_I \neq \nu_M$.

For homogeneous inclusion, $\alpha = 1$ and $\nu_I = \nu_M$, $C_1 = C_2 = 0$, $C_0 = C_3 = C_4 = C_5 = 1$, (3.23) returns to the well-known solution (Lambropoulos, 1986)

$$\frac{K_{tip}}{K} = 1 + \frac{\beta_3 + \beta_4 + \beta_5}{K} \tag{3.25}$$

The increment in K_{tip}, ΔK_{tip}, is given by

$$\Delta K_{tip} = \beta_3 + \beta_4 + \beta_5 \quad \text{for homogeneous inclusion} \tag{3.26}$$

and

$$\Delta K_{tip} = \Delta K_{tip}^m + \Delta K_{tip}^T \quad \text{for inhomogeneous inclusion} \tag{3.27}$$

where

$$\Delta K_{tip}^m = [C_0 - 1 + C_0(C_1\beta_1 + C_2\beta_2)]K \tag{3.28}$$

$$\Delta K_{tip}^T = C_0(C_3\beta_3 + C_4\beta_4 + C_5\beta_5) \tag{3.29}$$

ΔK_{tip}^m and ΔK_{tip}^T are the increments contributed by modulus toughening and transformation toughening, respectively. Both of them are dependent of the shape of the inclusion and the modulus difference between inclusion and matrix material. However, ΔK_{tip}^m is independent of the size of the inclusion and dependent of the applied stress intensity, while ΔK_{tip}^T is dependent on the size of the inclusion and independent of the applied stress intensity.

4. Applications

4.1. Pure modulus toughening

Because the fundamental formula (3.23) may return to the well-known theoretical solution for pure transformation toughening for homogeneous inclusion, the accuracy of the fundamental formula may be examined by the case of pure modulus toughening.

When the inherent transformation strains vanish, Eq. (3.23) becomes

$$\frac{K_{tip}}{K} = C_0(1 + C_1\beta_1 + C_2\beta_2) \tag{4.1}$$

corresponding to pure modulus contribution to crack tip field. An exact solution to circular inclusion centered at the tip of a semi-infinite crack is given by Steif (1987). For an inclusion with arbitrary shape, a close form solution to lowest order effect of the modulus difference between inclusion and matrix material is given by Hutchinson (1987). The model of circular inclusion centered at the tip of a semi-infinite crack is firstly used to measure the accuracy of (4.1). As shown in Fig. 3, good agreement between our solution and Steif's results is found. For comparison, the lowest order solution and the modified lowest order results

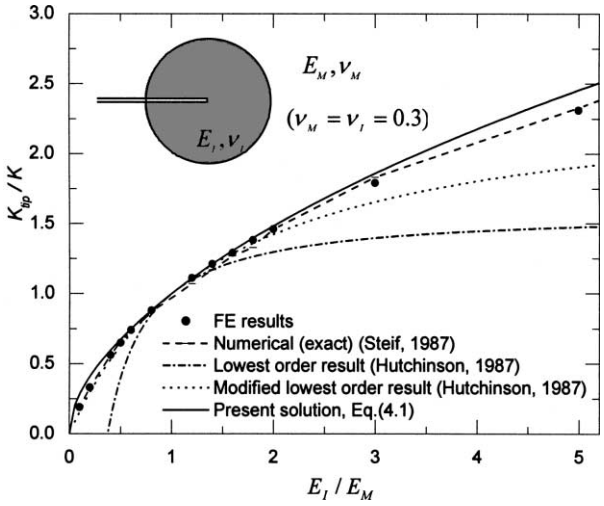

Fig. 3. A comparison of the selected results for a circular inclusion centered at crack tip.

(Hutchinson, 1987) are also plotted in Fig. 3. Though the agreement is good for the modified lowest order results when $E_I/E_M < 2$, it fails as E_I/E_M becomes larger than 2.

Detailed finite element (FE) analyses were also performed for this model. To calculate the K_{tip} in the FE-analyses, three J-integral contours within inclusion were set around crack-tip. The K_{tip} was calculated by (3.21) from the mean value of the three contours (note, in fact, that they nearly have no difference), J_{tip} . The K used to normalize K_{tip} is calculated for the mode of homogeneous matrix material at the same applied load. The FE-results are also plotted in Fig. 3. They are in excellent agreement with the exact solution obtained by Steif (1987). Therefore, the FE-analyses can be used to measure the accuracy of (4.1) for the inclusion with arbitrary shape.

Fig. 4 compares the results calculated from (4.1) and the modified lowest order solution (Hutchinson, 1987) with those obtained from FE-analyses for a square inclusion. The crack tip partially penetrates the

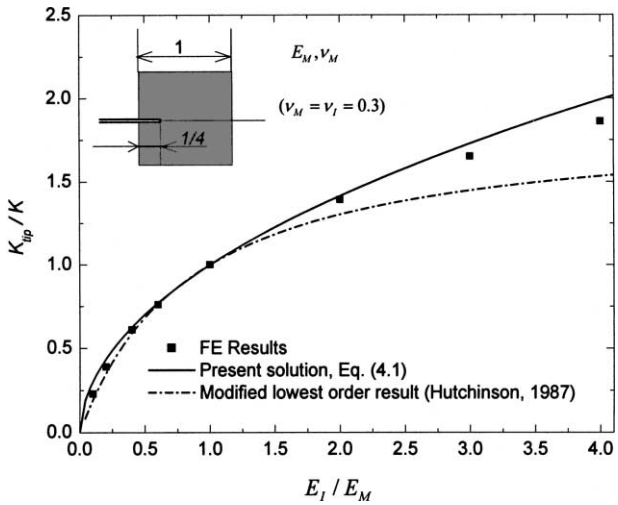

Fig. 4. A comparison of the results calculated from Eq. (4.1), the modified lowest order solution and FE-analyses for a square inclusion.

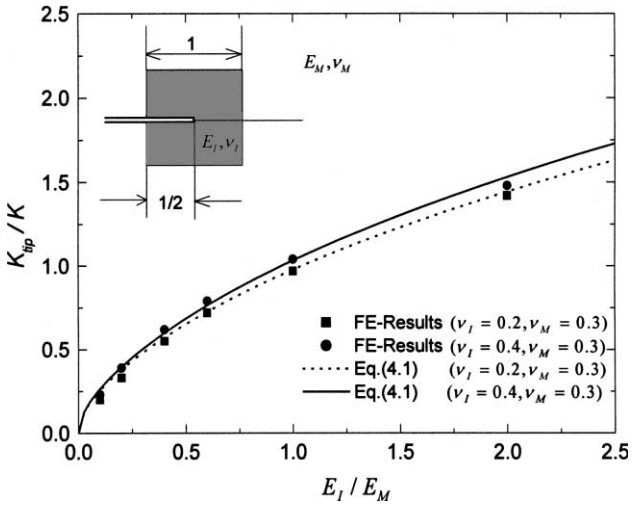

Fig. 5. A comparison of the results calculated from Eq. (4.1) and FE-analyses for a square inclusion in which both elastic modulus and Poisson's ratio differ from those of matrix material.

inclusion (1/4 edge length). As shown in Fig. 4 our results are in good agreement with those of the FE-analyses.

In Fig. 5, the value of K_{tip}/K for a square inclusion centered at crack tip predicted from (4.1) are compared with the results of FE-analyses for the case where v_{I} and v_{M} are different, and good agreement can be found.

4.2. Variation in SIF for a transformed particle

In this section, we assumed that an inclusion surrounding crack-tip undergoes a stress-free transformation strain, e^{T^*}, induced by phase transformation or thermal expansion mismatch.

Fig. 6 shows the ΔK_{tip} calculated from (3.27) as a function of $E_{\text{I}}/E_{\text{M}}$ for a crack partially penetrating a fibre shape inclusion with transformation strains $e_{11}^{\text{T}^*} = e_{22}^{\text{T}^*} = 0.02$ and $e_{12}^{\text{T}^*} = 0.04$. As shown in Fig. 6, both $K_{\text{tip}}^{\text{m}}$ and $K_{\text{tip}}^{\text{T}}$ are strongly dependent of the modulus ratio α, $K_{\text{tip}}^{\text{m}}$ increases, while $K_{\text{tip}}^{\text{T}}$ decreases, with increasing modulus ratio α.

The incremental transformation contribution predicted from present solution (3.29) is quite different that from previous analysis (3.26), which was derived based on homogeneous inclusion mode. One can introduce a parameter defined by

$$I = \frac{C_0(C_3\beta_3 + C_4\beta_4 + C_5\beta_5)}{\beta_3 + \beta_4 + \beta_5} \tag{4.2}$$

to measure the influence of modulus change on transformation toughening.

Fig. 7 shows the influence factor I for the calculation mode shown in Fig. 6 as a function of $E_{\text{I}}/E_{\text{M}}$ for different Poisson's ratios. This result clearly shows that the transformation toughening is strongly affected by modulus of the transformation zone. Therefore, the modulus change induced by phase transformation should be taken account in the calculation of transformation toughening. This situation has been overlooked in the previous study of transformation toughening.

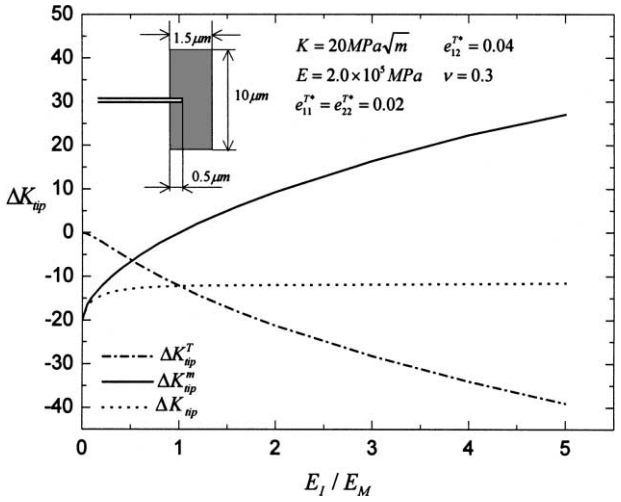

Fig. 6. ΔK_{tip} for a transformed fibre shape inclusion.

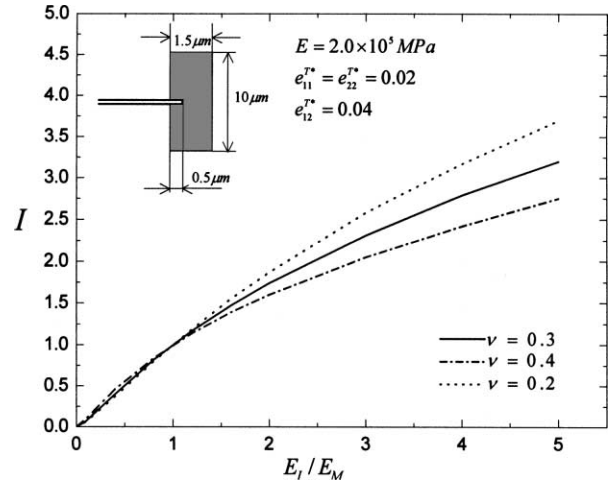

Fig. 7. Influence factor I as function of $E_{\text{I}}/E_{\text{M}}$ for different Poisson's ratio.

4.3. Microcrack toughening in brittle materials

Detailed numerical analysis for microcrack toughening has been performed by Hutchinson for several limited cases (Hutchinson, 1987). To compare with Hutchinson's results, the microcrack toughening effects were evaluated by the present solution to two specific shapes of microcrack zone dictated by two possible microcrack nucleation criteria. The first is based on the mean stress; the second is based on the maximum normal stress. In each case it was assumed that there is no preferred orientation to the microcracks so that the reduced moduli are isotropic and uniform. Results for both stationary cracks and cracks which have achieved steady-state growth conditions will be given so as to assess the potential for crack growth fol-

lowing initiation. In every example the zone shape and size are determined using the unperturbed elastic stress field controlled by the remote SIF K.

The modulus E_I and Poisson's ratio v_I of the micro-cracked material can be determined from Hutchinson (1987)

$$\frac{E_M}{E_I} = 1 + \frac{32}{45}\frac{(1-v_M)(5-v_M)}{(2-v_M)}f \tag{4.3}$$

$$v_I = v_M - \frac{16v_M}{15}\frac{(3-v_M)(1-v_M^2)}{(2-v_M)}f \tag{4.4}$$

$f = l^3N$ is the microcrack density parameter, as described by Budiansky and O'connell (1976), where l is the microcrack length and N the number density per unit volume. During microcrack opening, the release of residual stress σ_R will result in a dilatational strain θ^T that is given by Hutchinson (1987)

$$\theta^T = \frac{16}{3}(1-v_M^2)\frac{\sigma_R}{E_M}f \tag{4.5}$$

where $\theta^T = 1.5\ e_{ii}^{T^*}/(1+v_M)$ for plane strain, can be evaluated from the dilatational strains if desired. In the case of isotropic dilatation, the nonzero components of the dilatational strains are $e_{11}^{T^*}$ and $e_{22}^{T^*}$, and $e_{11}^{T^*} = e_{22}^{T^*}$ for plane strain. In this section, to compare with Hutchinson's results we use θ^T replacing the dilatational strains and the calculated results are limited to the lowest order effects of the microcrack density parameter f because it is small. Values of f about 0.3 near the crack tip have been observed (Ruehle et al., 1987).

4.3.1. Stationary and steadily growing crack with nucleation at a critical mean stress

With $\sigma_m = \sigma_{ii}/3$ as the mean stress, suppose a simplified nucleation criterion:

$$\begin{aligned} &f = 0 \quad \text{for} \quad (\sigma_m)_{max} < \sigma_m^c \\ &f = N \quad \text{for} \quad (\sigma_m)_{max} > \sigma_m^c \end{aligned} \tag{4.6}$$

where σ_m^c is the critical value at which microcrack nucleation is complete in the microcrack zone. The boundary of the microcrack zone A_c for stationary crack (Fig. 8) is given by

$$R(\theta) = \frac{2}{9\pi}(1+v_M)^2\left(\frac{K}{\sigma_m^c}\right)^2\cos^2\left(\frac{\theta}{2}\right) \tag{4.7}$$

As crack grows, a wake of microcrack zone is formed. The leading edge of the zone is given by (4.7) for $|\theta| < 60^0$, and the half-height of the zone, H is determined by (4.7) at $\theta = 60°$

$$H = \frac{\sqrt{3}(1+v_M)^2}{12\pi}\left(\frac{K}{\sigma_m^c}\right)^2 \tag{4.8}$$

Then, (3.28) and (3.29) give ($v_M = 1/3$)

$$\left.\begin{aligned} \Delta K_{tip}^m &= -0.72Kf \\ \Delta K_{tip}^T &= 0 \end{aligned}\right\} \tag{4.9}$$

for stationary crack, and

$$\left.\begin{aligned} \Delta K_{tip}^m &= -0.92Kf \\ \Delta K_{tip}^T &= -(0.32 - 0.47f)E\theta^T\sqrt{H} \end{aligned}\right\} \tag{4.10}$$

for steadily growing crack with the zone boundary specified by (4.7) for $|\theta| < 60°$ and by $|x_2| = H$ for $|\theta| > 60°$.

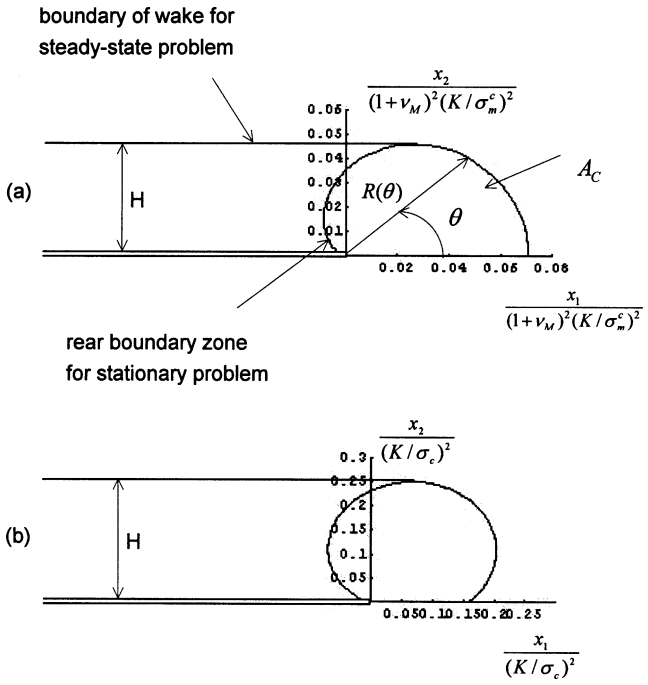

Fig. 8. Microcracked zones for stationary and steadily growing cracks for two nucleation criteria: (a) critical mean stress criterion, (b) critical maximum principal stress criterion.

4.3.2. Stationary and steadily growing crack with nucleation at a critical maximum normal stress

Now suppose that microcrack nucleation occurs when the maximum principal stress σ_1 reaches a critical value σ_c, i.e.

$$\begin{aligned} f &= 0 \quad \text{for} \quad (\sigma_1)_{\max} < \sigma_c \\ f &= N \quad \text{for} \quad (\sigma_1)_{\max} > \sigma_c \end{aligned} \tag{4.11}$$

where, as before, $()_{\max}$ signifies the maximum value attained over the history. The boundary of A_c for stationary crack is determined by

$$R(\theta) = \frac{1}{2\pi}\left(\frac{K}{\sigma_c}\right)^2\left(\cos\frac{\theta}{2} + \frac{1}{2}\sin|\theta|\right)^2 \tag{4.12}$$

and this is shown in Fig. 8(b). The half-height of A_c is obtained at $\theta = 74.84°$ and is

$$H = 0.2504\left(\frac{K}{\sigma_m^c}\right)^2 \tag{4.13}$$

Then, Eq. (3.28) and (3.29) give ($\nu_M = 1/3$)

$$\left.\begin{aligned} \Delta K_{\text{tip}}^{\text{m}} &= -0.82Kf \\ \Delta K_{\text{tip}}^{\text{T}} &= -(0.15 - 0.18f)E\theta^{\text{T}}\sqrt{H} \end{aligned}\right\} \tag{4.14}$$

for stationary crack.

For steadily growing crack, the zone A_c is specified by (4.12) for $|\theta| < 74.84°$ and by $|x_2| = H$ for $|\theta| > 74.84°$. Thus, Eq. (3.28) and (3.29) give

Table 1
Comparisons between the present solution and Hutchinson's results for two microcracking nucleation criteria. The values of ΔK_{tip} are calculated from $\nu_M = 1/3$ to the lowest order effect of the microcrack density f

Nucleation criterion	Crack	ΔK_{tip}	Present solution	Hutchinson's solution
Criticial mean stress $\sigma_m = \sigma_m^c$	Stationary crack	ΔK_{tip}^m	$-0.72Kf$	$-0.92Kf$
		ΔK_{tip}^T	0	0
	Steady-state crack	ΔK_{tip}^m	$-0.92Kf$	$-1.28Kf$
		ΔK_{tip}^T	$-(0.32-0.47f)E\theta^T\sqrt{H}$	$-0.32E\theta^T\sqrt{H}$
Criticial maximun mean stress $\sigma_1 = \sigma_c$	Stationary crack	ΔK_{tip}^m	$-0.82Kf$	$-1.15Kf$
		ΔK_{tip}^T	$-(0.15-0.18f)E\theta^T\sqrt{H}$	$-0.16E\theta^T\sqrt{H}$
	Steady-state crack	ΔK_{tip}^m	$-0.97Kf$	$-1.42Kf$
		ΔK_{tip}^T	$-(0.4-0.48f)E\theta^T\sqrt{H}$	$-0.4E\theta^T\sqrt{H}$

$$\left.\begin{aligned}\Delta K_{tip}^m &= -0.97Kf\\ \Delta K_{tip}^T &= -(0.4-0.48f)E\theta^T\sqrt{H}\end{aligned}\right\} \tag{4.15}$$

All the results for the two models have been assembled in Table 1, and compared with Hutchinson's results (1987). While the two models give similar results both for our and Hutchinson's analyses, the difference between our and Hutchinson's results are appreciable. The difference stems from two sources: One is the modulus toughening. Our solution is not limited to lowest order effect of modulus ratio between inclusion and matrix material. Hence, it will, as shown in Figs. (3) and (4), give more exact prediction than the lowest order accuracy. The other is the transformation toughening. Our solution has been taken account for the influence of the modulus change in transformation zone on the transformation toughening which has been overlooked in previous analysis. As shown in Table 1, the transformation contribution is weakened by microcracking. This result is reasonable because at the same dilatational strain level a soft transformation zone will produce lower compressive stress than hard one.

5. Conclusions and discussions

When a crack is lodged in an inhomogeneous inclusion, a transformation or microcrack process zone, the modulus variation and stress-free transformation strain in which will change the near-tip field of the crack. A close form of solution for predicting the toughening (or amplification) effect contributed from modulus variation and transformation strain, as well as interaction between them is derived based on Eshelby equivalent inclusion approach. The solution is accurate, as validated by several numerical examples, and provides a quick estimate for the effects of shape, size, and stiffness of an inclusion or a process zone surrounding crack-tip on the crack-tip field.

The limitation of the solution is that the remote K-field was used to calculate the equivalent transformation strain of the inclusion or process zone. Hence, the size of the inclusion or process zone must be small compared with the length of crack and other dimensions of the cracked body.

References

Budiansky, B., O'connell, R.J., 1976. Elastic moduli of cracked solid. International Journal of Solids and Structures 12, 240–245.
Budiansky, B., Hutchinson, J.W., Lambropoulos, J.C., 1983. Continuum theory of dilatant transformation toughening in ceramics. International Journal of Solids and Structures 19, 337–355.

Clussen, N., Ruehle M., Heuer, H., 1984. Science and Technology of Zirconia II. In: Advances in Ceramices, vol. 12. American Ceramic Society, Columbus, OH.

Eshelby, J.D., 1957. The determination of the elastic fields of an ellipsoidal inclusion, and related problems. In: Proceedings of the Royal Society, vol 241. London, Series A, pp. 376–396.

Evans, A.G., Cannon, R.M., 1986. Toughening of brittle solids by martensitic transformations. Acta Metallurgica Materialia 34, 761–800.

Evans, A.G., Faber, K.T., 1986. Toughening of ceramics by circumferential microcracking. Journal of the American Ceramic Society 64, 394–398.

Evans, A.G., Mater, 1988. High toughness ceramics. Materials Science and Engineering A105/106, 65–75.

Hoaland, R.G., Embury, J.D., 1980. A treatment of inelastic deformation around a crack tip due to microcracking. Journal of the American Ceramic Society 63, 404–410.

Hueber, H., Jillek, W., 1977. Sub-critical crack extension and crack resistance in polycrystalline alumina. Journal of Materials Science 12, 117–125.

Hutchinson, J.C., 1987. Crack tip shielding by micro-cracking in brittle solids. Acta Metallurgica Materialia 35, 1605–1619.

Johnson, W.C., Earmme, Y.Y., Lee, J.K., 1980. Approximation of the strain field associated with an inhomogeneous precipitate. Journal of Applied Mechanics 47, 775–780.

Knehans, R., Steinbrech, R., 1982. Memory effect of crack resistance during slow crack growth in notched Al_2O_3 bend specimens. Journal of Materials Science Letters 1, 327–331.

Kriven, W.M., 1990. Martensitic toughening of ceramics. Materials Science and Engineering A127, 249–255.

Lambropoulos, J.C., 1986. Shear, shape and orientation effects in transformation toughening in ceramics. International Journal of Solids and Structures 22, 1083–1106.

McMeeking, R.M., Evans, A.G., 1982. Mechanics of transformation toughening in brittle materials. Journal of the American Ceramic Society 65, 242–246.

Moschobidis, Z.A., Mura, T., 1975. Two ellipsoidal inhomogeneities by the equivalent inclusion method. ASME Journal of Applied Mechanics 42, 847–852.

Mura, T., 1987. Micromechanics of Defects in Solids. Second Revised Edition, Dordrecht.

Ruehle, M., Evans, A.G., McMeeking, R.M., Charalambiders, P.G., Hutchinson, J.W., 1987. Acta Metallurgica Materialia 35, 2701–2710.

Steif, P.S., 1987. A semi-infinite crack partially penetrating a circular inclusion. Journal of Applied Mechanics 54, 87–92.

Taya, M., Chou, T.W., 1981. On two kinds ellipsoidal inhomogeneities in an infinite elastic body: an application to a hybrid composites. International Journal of Solids and Structures 17, 553–563.

Withers, D.J., Stobbs, W.M., Pederson, O.B., 1989. The application of the eshelby method of internal stress determination to short fibre metal matrix composites. Acta Metallurgica Materialia 37, 3061–3084.